http://dx.doi.org/10.5012/bkcs.2012.33.2.583

Solution Structure of LXXLL-related Cofactor Peptide of Orphan Nuclear Receptor FTZ-F1

Ji-Hye Yun, Chul-Jin Lee, Jin-Won Jung, and Weontae Lee*

Department of Biochemistry, College of Life Science and Biotechnology, Yonsei University, Seoul 120-749, Korea
**E-mail: wlee@spin.yonsei.ac.kr*
Received November 9, 2011, Accepted December 15, 2011

Functional interaction between *Drosophila* orphan receptor FTZ-F1 (NR5A3) and a segmentation gene product *fushi tarazu* (FTZ) is crucial for regulating genes related to define the identities of alternate segmental regions in the Drosophila embryo. FTZ binding to the ligand-binding domain (LBD) of FTZ-F1 is of essence in activating its transcription process. We determined solution structures of the cofactor peptide (FTZ^{PEP}) derived from FTZ by NMR spectroscopy. The cofactor peptide showed a nascent helical conformation in aqueous solution, however, the helicity was increased in the presence of TFE. Furthermore, FTZ^{PEP} formed α-helical conformation upon FTZ-F1 binding, which provides a receptor bound structure of FTZ^{PEP}. The solution structure of FTZ^{PEP} in the presence of FTZ-F1 displays a long stretch of the α-helix with a bend in the middle of helix.

Key Words : *Fushi tarazu*, FTZ-F1, Cofactor, NMR, LXXLL motif

Introduction

Fushi tarazu factor 1 (FTZ-F1) is an orphan nuclear receptor that interact with FTZ to define identities of alternate segmental regions in Drosophila embryo.[1,2] FTZ-F1 has two conserved structural features; DNA-binding domain (DBD) consists of two zinc fingers and a putative ligand-binding domain (LBD) is located at the C-terminal region.[3]

In ligand-dependent NRs, various lipophilic ligands interact with the apo-type receptors, converting them into an active holo-type[4-9] leading to transcriptional activation[10,11] or repression.[12,13] The binding of the ligand to the ligand-binding pocket induces allosteric changes in the configuration of helix 12 (AF-2 helix). However, the cognate ligand of FTZ-F1 has not yet been identified and the molecular mechanisms of their transcriptional regulation remain unclear. In contrast to ligand-dependent transcriptional activation, the C-terminal activation helix (AF-2) of the orphan receptor mLRH-1is positioned in an active conformation to accommodate co-regulator binding in spite of the large ligand-binding pocket.[14] In the nuclear receptor superfamily, FTZ-F1 is most homologous to LRH-1. The FTZ-F1 and LRH-1 share well-conserved ligand-binding domain (40% identity) that interacts with their co-regulators. In addition, FTZ-F1 constitutively interacts with FTZ co-activator in the absence of any exogenous ligands.[15] Thus, the AF-2 of orphan receptor FTZ-F1 seems to have its active conformation similar to that of LRH-1.

FTZ-F1 acts as an activator of the pair-rule class segmentation gene *fushi tarazu* (*ftz*).[16] In blastoderm embryos, FTZ-F1 is uniformly expressed, whereas FTZ is expressed as seven stripes in the even-numbered parasegments,[17] ftz is required for formation of these parasegments and thus *ftz* mutant embryos possess only half of the normal number of body segments.[18] FTZ contains a highly conserved homeodomain that is required for DNA binding activity.[19] Interestingly, FTZ can perform some of its regulatory functions in the absence of its homeodomain, interacting with FTZ-F1 as co-activator.[20] Thus, FTZ and FTZ-F1 cooperate to regulate target gene expression. Most transcriptional co-activators including FTZ have been shown to regulate transcriptional signals through binding to nuclear receptors using conserved LXXLL-related motifs (NR boxes). LXXLL co-activator motifs interact with helices 3, 4, and 12 (AF-2) in the LBD of nuclear receptors. It is especially important that the helix AF-2 is appropriately realigned.[21,22] FTZ-F1 also contains a highly conserved AF-2 motif, which is shown to be crucial for interactions with FTZ *in vitro* and *vivo*. The LXXLL motif of FTZ closely resembles AF-2 helixes that are found in most transcriptional co-regulators interacting with the LBDs of nuclear receptors.[23] Thus, it is assumed that FTZ uses the same LXXLL-related motifs to interact with FTZ-F1. Recently, our laboratory reported the structural basis for the FTZ-F1/FTZ interaction by X-ray crystallography,[3] however, the cofactor peptide shows a short helical structure. To gain further insight into the structural properties of the cofactor peptide in solution state, we have performed NMR studies on a synthetic peptide containing LXXLL-related motifs of FTZ, which is corresponding to FTZΔ112-120 (FTZ^{PEP}).

Materials and Methods

Protein Preparation and Peptide Synthesis. Protein expression of the Drosophila FTZ-F1 was induced in BL21(DE3) E. coli with 0.25 mM IPTG followed by growth at 25 °C for 6 hr. IPTG-induced cells were harvested by

centrifugation at 4 °C. Pellets were resuspended in buffer [25 mM sodium phosphate (pH 7.0), 300 mM NaCl and 10 mM DTT] and then broken by sonication. The supernatants were collected by ultracentrifugation (140000 g for 30 min at 4 °C) to remove the membrane fraction. His-tagged FTZ-F1 LBD protein was then applied to TALON (BD Biosciences) column. The resin was washed extensively with washing buffer [25 mM sodium phosphate (pH 7.0), 300 mM NaCl, 10 mM DTT and 30 mM imidazole] to remove nonspecifically bound proteins. His-tagged FTZ-F1 LBD protein was eluted with elution buffer [25 mM sodium phosphate (pH 7.0), 300 mM NaCl, 10 mM DTT and 250 mM imidazole]. His-tagged FTZ-F1 LBD protein was purified on a TALON (BD Biosciences) column and eluted in 300 mM of imidazole. After removal of the His-tag with bovine thrombin (Amersham Biosciences), protein was further purified by gel filtration on Superdex 75 (Amersham Biosciences). Uniformly ^{15}N-labeled protein samples were prepared by growing the cells in M9 minimal medium containing $^{15}NH_4Cl$ (Cambridge Isotope Laboratories, Inc.). For residue-specific ^{15}N-labeling of leucine, the protein was expressed in the leucine-auxotrophic strain DL39 (DE3) using M9 minimal medium supplemented with [^{15}N]-leucine (Cambridge Isotope Laboratories, Inc.). Uniformly [90% ^{2}H/^{13}C/^{15}N]- labeled protein samples were prepared by growing cells in the D_2O M9 minimal media containing $^{15}NH_4Cl$ and $^{13}C_6$-D-glucose as the sole source of nitrogen and carbon. FTZ^{PEP} was synthesized commercially by Anygen Co. (Kwangju, Korea). FTZ^{PEP} was characterized by high pressure liquid chromatography and mass spectrometry. The purity of the peptides was greater than 98% as determined by these methods.

CD Experiments. Circular dichroism has been performed on a J-810 instrument (JASCO) at 25 °C. A 0.1 cm quartz cuvette was used for CD experiments. Each of the CD spectra was obtained from an average of 10 accumulations with step resolution of 0.2 nm and 2.0 nm bandwidth. The spectra were recorded from 180 to 250 nm at scanning rate of 50 nm/min with a time constant of 0.5 s. The signal of FTZ-F1 was subtracted from the signal of the FTZ^{PEP}/FTZ-F1 complex. A standard noise reduction was performed on the final spectrum. The samples contained 40 μM peptide or the peptide/protein complex, 25 mM sodium phosphate, various concentrations of TFE at pH 7.0. The secondary structure content was estimated from the CD spectra according to the methods of CONTIN-LL, SELCON3, and CDSSTR.

NMR Experiments. Samples for NMR experiments contained 0.25 mL of 2 mM concentration of peptide in 25 mM sodium phosphate buffer at 6.5 pH in 90% H_2O/10% D_2O solution and in 50% H_2O/50% 2,2,2-trifluoro-(d3)-ethanol (TFE) mixture (v/v). The peptide/protein complex sample was prepared by titrating FTZ^{PEP} into ^{15}N-labeled FTZ-F1 sample. For NOE measurements of the peptide bound to FTZ-F1, the peptide/deuterated-protein complex sample was prepared. NMR spectra were recorded and 25 °C on Bruker DRX-500 and DMX-600 spectrometers equipped with a triple-resonance probe with pulsed-field gradient coil. Two-dimensional (2D) NMR spectra were recorded in phase-sensitive mode using time-proportional phase incrementation[24] for quadrature detection in the t_1 domain. The 2D experiments such as double-quantum-filtered COSY (DQF-COSY),[25] TOCSY using a MLEV-17 spin-lock pulse sequence with a mixing time of 69.7 ms, and NOESY with mixing times ranging between 200-600 ms were performed. For DQF-COSY experiments, solvent suppression was achieved using selective low-power irradiation of the water resonance during 2.0 s of relaxation delay. Solvent suppression for TOCSY and NOESY experiments was achieved using a WATERGATE pulse sequence[26] combined with pulsed-field gradient pulses. All NMR spectra were acquired with 2048 complex data points in t_2 and 256 increments in the t_1 domain. The $^{3}J_{HN\alpha}$ coupling constants were measured from 2D-DQF-COSY spectra, strip-transformed to 8 K × 1 K. NMR data were processed on a Silicon Graphics Indigo2 workstation using nmrpipe/nmrdraw (Biosym/Molecular Simulations, Inc., San Diego, CA, USA) or Xwinnmr (Bruker Instruments, Karlsruhe, Germany) software and analyzed using the Sparky 3.95 program. The proton chemical shifts were referenced with internal sodium 2,2-dimethyl-2-silapentane 1-sulfonate (DSS).

Structure Calculations. Distance restraints were derived from the 400-ms NOESY spectra recorded in 90% H_2O/10% D_2O, 90% H_2O/10% D_2O with FTZ-F1 and 50% TFE/40% H_2O/10% D_2O mixture at pH 6.5, 5 °C, respectively. Constraints for the dihedral angles were deduced on the basis of the $^{3}J_{HN\alpha}$ coupling constants from both proton 1D and 2D DQF-COSY spectrum. The solution structures were calculated by the distance geometry and dynamic simulated annealing (SA) procedures with the CNS 1.1 program. The methodology employed is similar to a previously reported protocol.[27] The target function for molecular dynamics and energy minimization consisted of a covalent structure, van der Waals repulsion, NOE and torsion angle constraints. Based on cross peak intensities on the NOESY spectra with mixing times of 200-600 ms, the distance constraints were classified into three distance categories; strong (0.18-0.27 nm), medium (0.18-0.33 nm) and weak (0.18-0.5 nm). Pseudo-atom corrections were used for non-stereospecifically assigned methylene protons, methyl groups and the aromatic phenylalanine protons.[28] Backbone dihedral restraints inferred from $^{3}J_{HN\alpha}$ coupling constants were used as -55 ± 45^{o} for a $^{3}J_{HN\alpha}$ less than 6 Hz and -120 ± 50^{o} for a $^{3}J_{HN\alpha}$ greater than 8 Hz. Final structures are displayed using Pymol programs.

Results and Discussion

CD Spectroscopy. CD spectra were acquired on FTZ^{PEP} in various concentrations of TFE. Figure 1(a) shows that the peptide contained a small population of helical conformation in water. However, the helical structure was induced upon addition of TFE solution. FTZ^{PEP} showed a maximum helicity in 60% TFE solution. We performed CD experiments on peptide/protein complex at 1:1 and 1:2 molar ratio [FTZ^{PEP}:

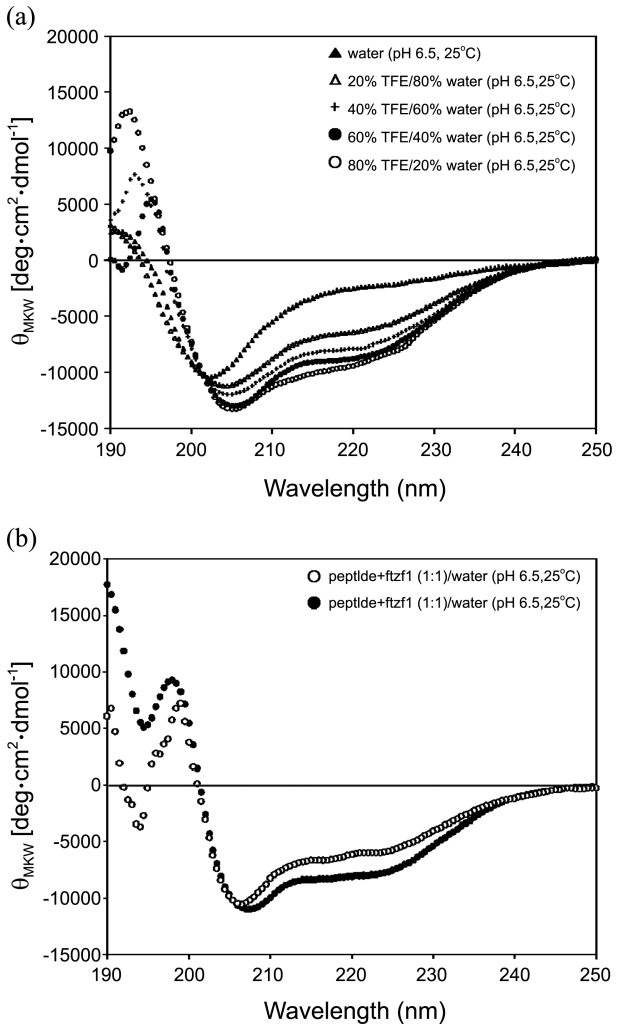

Figure 1. Circular dichroism spectra of 40 μM FTZ^{PEP}(pH 6.5, 25 °C) (a) in various TFE concentrations; in water (closed triangles), 20% TFE/80% water (open triangles), 40% TFE/60% water (cross bars), 60% TFE/40% water (closed circles) and 80% TFE/20% water (open circles), and (b) in the presence of 40 μM (closed circles), 80 μM Ftz-f1 LBD (open circles). The secondary structure composition was estimated by deconvolution, as implemented by the CDPro software. *The ellipticity of Ftz-f1 was removed in (b).

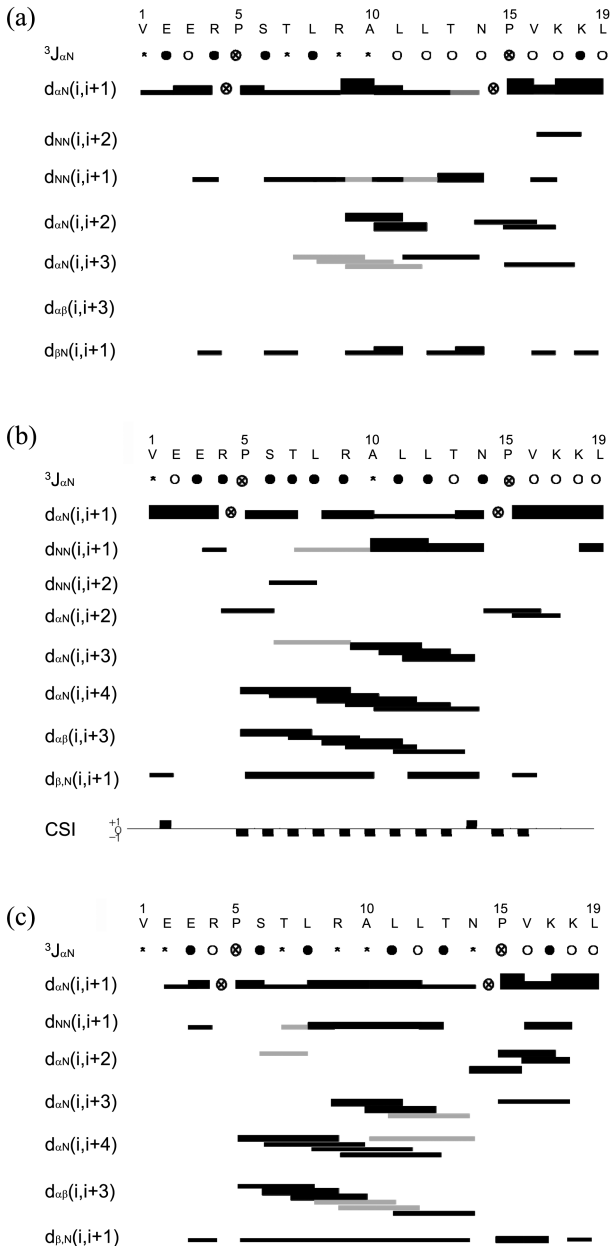

Figure 2. Summary of NMR data for FTZ^{PEP} in (a) 90% H_2O/10% D_2O at pH 6.5, 5 °C, (b) 90% H_2O/10% D_2O at pH 6.5, 25 °C with FTZ-F1 and (c) 50% TFE/40% H_2O/10% D_2O mixture at pH 6.5, 25 °C showing the sequential and short-range NOE contacts. Backbone vicinal coupling constants (closed circle: $^3J_{NH\alpha} < 6$ Hz, *means unresolved and ambiguous ones), chemical shift indices (CSI) calculated for for Hα, Hβ, Cα are also indicated. ⊗ is represented the proline residues. The gray line represents the unresolved from the resonance overlapping.

FTZ-F1] (Fig. 1(b)). To obtain CD spectra of the bound peptide, the signal of FTZ-F1 was subtracted from the signal of the peptide/protein complex. We found that FTZ^{PEP} forms a helical conformation in the presence of FTZ-F1. This result supports that the FTZ^{PEP} forms a helix upon receptor binding. FTZ^{PEP} could be stabilized both in TFE solution and in the presence of FTZ-F1 and a helical conformation is important for FTZ-F1 binding. The helicity of FTZ^{PEP} in the 1:2 molar ratio is lower than that of 1:1 (Fig. 1(b)). This might be due to contribution of the free peptide because the binding affinity of the FTZ^{PEP} is relatively weak (K_d = 1.52 uM).[3]

Solution Structures of FTZ^{PEP}. Complete proton resonance assignments of the FTZ^{PEP} in the absence of FTZ-F1, in 50% TFE solution and in the present of FTZ-F1 were achieved using the standard resonance assignment procedure.[31] Once the individual spin systems had been classified, backbone sequential resonance assignments were easily completed by $d_{\alpha N}$ (i, i + 1) NOE connectivities in the 2D-NOESY spectra. Overlapped in amide-amide region of the peptide/protein complex NOESY spectra, the NOE peaks could be resolved using F2/F1 ^{15}N filtered experiment. Figure 2 summarizes the sequential and short-range NOE connectivities observed for FTZ^{PEP} in the absence of FTZ-F1, in the present of FTZ-F1 and in 50% TFE solution. We

Table 1. Summary of NOE distance restraints and structural statistics for FTZ^{PEP}

	FREE (H_2O)		FREE (TFE)		FTZ-F1 BOUND	
Number of distance restraints						
Total	186		227		248	
Intraresidue	111		127		138	
Sequential (| i – j | = 1)	39		43		48	
Short range (1 < | i – j | ≤ 5)	36		57		62	
Number of dihedral angle restraints	13		15		12	
Atomic rmsd from average						
Backbone atoms (Å)	2.08		0.54		0.43	
All atoms (Å)	3.66		1.44		1.79	
	<SA>k	<SA>kr	<SA>k	<SA>kr	<SA>k	<SA>kr
Energies						
Total (Kcal·mol^{-1})	27.74	20.37	43.37	41.94	30.09	17.26
Bonds (Kcal·mol^{-1})	0.25	0.11	3.51	3.26	0.4476	0.33
Angles (Kcal·mol^{-1})	15.52	15.31	21.4	20.79	17.34	16.04
Van der Waals (Kcal·mol^{-1})	0.78	0.13	4.947	4.656	7.367	0.03
NOE (Kcal·mol^{-1})	11.72	3.86	12.98	10.81	4.367	0.6533
Lennard-Jones[a] (Kcal·mol^{-1})	-43.12	-48.33	-50.21	-51.3	-58.21	-73.38
Deviations from ideal geometry						
Bonds (Å)	0.0009	0.0008	0.0033	0.0029	0.0015	0.0010
Angles (deg)	0.4463	0.4193	0.4995	0.4369	0.4476	0.4173
Impropers (deg)	0.1048	0.1014	0.2838	0.2374	0.1632	0.1076

[a]Lennard-Jones is the Lennard Jones/van der Waals potential calculated using CHARMm empirical energy function.

could observe continuous d_{NN} (i, i + 1) contacts together with the characteristic $d_{\alpha N}$ (i, i + 3), $d_{\alpha N}$ (i, i + 4) and the $d_{\alpha b}$ (i, i + 3) NOEs for FTZ^{PEP}. These results strongly support that FTZ^{PEP} in the absence of FTZ-F1 contains a small population of helical conformation due to intrinsic dynamics nature of small peptide. However, FTZ^{PEP} has a high population of helical conformation both in 50% TFE solution and in the present of FTZ-F1. The observation of intense $d_{\alpha N}$ (i, i + 3), $d_{\alpha N}$ (i, i + 4) and the $d_{\alpha b}$ (i, i + 3) NOEs (Fig. 2(b)) supports that FTZ^{PEP} in 50% TFE solution forms an α-helix. FTZ^{PEP} forms an α-helix comprising residue –3 Pro- +11 Lys in the present of FTZ-F1 (Fig. 2(c)). This result is further supported by the small $^3J_{HN\alpha}$ coupling constants. Chemical shift index values are also indicative of the helical conformation. The NMR structures for FTZ^{PEP} were calculated using the experimental restraints derived from 2D-NOESY and DQF-COSY spectra. A total of 30 distance geometry structures served as starting structures for dynamical simulated-annealing calculations for the peptide in both water and TFE solutions. All 30 structures showed no restraint violations greater than 0.03 nm for distances and 38 for torsion angles. The 25 lowest-energy structures (<SA>k) of 30 simulated annealing structures were selected for detailed structural analysis. The average structure was calculated from the geometrical average from 25 <SA>k structure coordinates and subjected to restraint energy minimization to correct covalent bonds and angle distortions. Energies and structural statistics for 25 <SA>k and <SA>kr structures are listed in Table 1. A best-fit superposition of 20 <SA>k structures along with the energy minimized average struc ture (<SA>kr) is shown in Figure 3. In the absence of FTZ-F1, FTZ^{PEP} shows a nascent helical structure (Fig. 3(a)). FTZ^{PEP} in solution has fewer NOEs, resulting high rmsd for backbone atoms. This result suggests that FTZ^{PEP} is dynamic in water solution. However, FTZ^{PEP} have intense helical NOEs in TFE solution, indicating an α-helical conformation (Fig. 3(b)). FTZ^{PEP} in the complexed with FTZ-F1 forms an α-helix spanning residues from –3 Pro to +11 Lys. Interestingly, the helix is bent (< 20-40) near proline residue at +8 position (Fig. 3(e)).

Previous studies showed that the NR box motif of FTZ, containing LRALLT sequence which is closely flanked by proline residues on each side, is required for interact with FTZ-F1 *in vitro*,[20] and a conserved AF-2 motif is essential for contact with FTZ and for FTZ-F1 function in vivo. The present paper supplements these earlier observations with physicochemical data on the interaction of FTZ-F1 and FTZ NR box in solution state. CD spectra of the FTZ^{PEP} at different TFE concentrations and in the present of FTZ-F1 LBD demonstrated that the helical structure of FTZ^{PEP} is induced in TFE solution. It is noteworthy that the secondary structure composition of FTZ^{PEP} in 40% TFE solution is very close to that in the presence of FTZ-F1 LBD. This result implies that FTZ^{PEP} binds to the FTZ-F1 with a helical

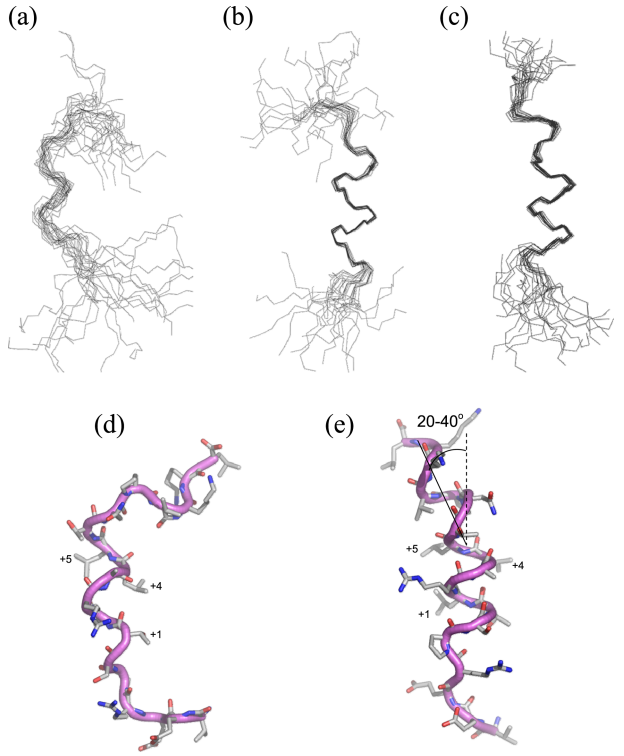

Figure 3. NMR structures of both free and FTZ-F1 bound FTZ^{PEP}. Superposition of the final 20 low energy structures of FTZ^{PEP} displayed. Solution structures of FTZ^{PEP} are shown. (a) in H_2O solution, (b) in TFE mixture, (c) in the presence FTZ-F1 LBD. Ribbon diagrams of each representative structure from REM structures of FTZ^{PEP} are shown (d) in water and (e) in the presence of Ftz-F1 LBD.

conformation. NMR structures of FTZ^{PEP} coincide with that of CD experiments that describe that the FTZ^{PEP} contains a helical conformation both in TFE solution and in the presence of FTZ-F1. Through the structural analysis by NMR, we verified that in the free FTZ^{PEP} shows the nascent helical structure (Fig. 3(a)), whereas the main secondary-structural feature of the bound FTZ^{PEP} is α-helix spanning from –3 Pro to +11 Lys (Fig. 3(c)). In the bound structure of FTZ^{PEP}, the LXXLL motif appears to be a well-defined hydrophobic region which consists of three leucines of the motif. The region forms hydrophobic interaction with the receptor so that the peptide becomes more compact and more stable in the bound state than in free one.

Although the FTZ^{PEP} seems to use the same LXXLL-related motif to interact with FTZ-F1, the interaction between the FTZ-F1 and FTZ^{PEP} contains three specific interactions to stabilize the complex based on our previous data from X-ray crystallography.[3] First, FTZ-F1's K855 interact with the main chain oxygen atom of FTZ^{PEP}'s +5 Pro as if the positive charge clamp (R849) form polar contact with backbone carbonyl group. Second, FTZ-F1's E1019 equivalent to negative charge clamp interacts with positively charged side chain of FTZ^{PEP}'s –4 Arg. Third, another aginine side chain at +2 position in the FTZ^{PEP} is involved in a polar contact with D860 of FTZ-F1. These unique interactions may allow FTZ-F1 to respond selectively to the FTZ^{PEP} containing NR box motif. In previous studies, it was reported that the selective binding of the co-regulator peptides to the receptors is achieved by the specific structural features of the LBD and NR box motif.[15] Therefore, atypical interactions in many other NR/co-regulator complexes seem to vary selectivity and affinity of co-regulator including LXXLL motif to respond various transcriptional signals. Our present study supports that the orphan nuclear receptor FTZ-F1 uses an additional charge clamp and specific polar contacts for binding to the FTZ^{PEP} including LXXLL motif in solution phase.

Conclusion

We determined solution structures of the cofactor peptide (FTZ^{PEP}) of both free and receptor bound state by NMR spectroscopy. The structure shows a nascent helical conformation in aqueous solution, however, a long stretch of α-helix forms in the presence of TFE and receptor protein, mimicking its native structure. The solution structure of FTZ^{PEP} in the presence of receptor FTZ-F1 displays an α-helix with a bend near proline at +8 position.

Acknowledgments. This research was supported by WCU (World Class University) program (R33-2009-000-10123-0, W. L.) and by the Brain Korea 21 (BK21) program of the National Research Foundation of Korea.

References

1. Guichet, A.; Copeland, J. W.; Erdelyi, M.; Hlousek, D.; Zavorszky, P.; Ho, J.; Brown, S.; Percival-Smith, A.; Krause, H. M.; Ephrussi, A. *Nature* **1997**, *385*(6616), 548-552.
2. Yu, Y.; Li, W.; Su, K.; Yussa, M.; Han, W.; Perrimon, N.; Pick, L. *Nature* **1997**, *385*(6616), 552-555.
3. Yoo, J.; Ko, S.; Kim, H.; Sampson, H.; Yun, J.-H.; Choe, K.-M.; Chang, I. S.; Lee, W. *J. Biol. Chem.* **2011**, *286*(36), 31225-31231.
4. Kastner, P.; Mark, M.; Chambon, P. *Cell* **1995**, *83*(6), 859-869.
5. Mangelsdorf, D. J.; Evans, R. M. *Cell* **1995**, *83*(6), 841-850.
6. Mangelsdorf, D. J.; Thummel, C.; Beato, M.; Herrlich, P.; Schutz, G.; Umesono, K.; Blumberg, B.; Kastner, P.; Mark, M.; Chambon, P.; Evans, R. M. *Cell* **1995**, *83*(6), 835-839.
7. Thummel, C. S. *Cell* **1995**, *83*(6), 871-877.
8. Blumberg, B.; Evans, R. M. *Genes Dev.* **1998**, *12*(20), 3149-3155.
9. Giguere, V. *Endocr. Rev.* **1999**, *20*(5), 689-725.
10. Bourguet, W.; Ruff, M.; Chambon, P.; Gronemeyer, H.; Moras, D. *Nature* **1995**, *375*(6530), 377-382.
11. Renaud, J. P.; Rochel, N.; Ruff, M.; Vivat, V.; Chambon, P.; Gronemeyer, H.; Moras, D. *Nature* **1995**, *378*(6558), 681-689.
12. Brzozowski, A. M.; Pike, A. C.; Dauter, Z.; Hubbard, R. E.; Bonn, T.; Engstrom, O.; Ohman, L.; Greene, G. L.; Gustafsson, J. A.; Carlquist, M. *Nature* **1997**, *389*(6652), 753-758.
13. Shiau, A. K.; Barstad, D.; Loria, P. M.; Cheng, L.; Kushner, P. J.; Agard, D. A.; Greene, G. L. *Cell* **1998**, *95*(7), 927-937.
14. Sablin, E. P.; Krylova, I. N.; Fletterick, R. J.; Ingraham, H. A. *Mol. Cell* **2003**, *11*(6), 1575-1585.
15. Suzuki, T.; Kasahara, M.; Yoshioka, H.; Morohashi, K.; Umesono, K. *Mol. Cell Biol.* **2003**, *23*(1), 238-249.
16. Ueda, H.; Sonoda, S.; Brown, J. L.; Scott, M. P.; Wu, C. *Genes Dev.* **1990**, *4*(4), 624-635.
17. Carroll, S. B.; Scott, M. P. *Cell* **1985**, *43*(1), 47-57.
18. Wakimoto, B. T.; Turner, F. R.; Kaufman, T. C. *Dev. Biol.* **1984**, *102*(1), 147-172.

19. Desplan, C.; Theis, J.; O'Farrell, P. H. *Cell* **1988**, *54*(7), 1081-1090.
20. Schwartz, C. J.; Sampson, H. M.; Hlousek, D.; Percival-Smith, A.; Copeland, J. W.; Simmonds, A. J.; Krause, H. M. *Embo. J.* **2001**, *20*(3), 510-519.
21. Feng, W.; Ribeiro, R. C.; Wagner, R. L.; Nguyen, H.; Apriletti, J. W.; Fletterick, R. J.; Baxter, J. D.; Kushner, P. J.; West, B. L. *Science* **1998**, *280*(5370), 1747-1749.
22. Mak, H. Y.; Hoare, S.; Henttu, P. M.; Parker, M. G. *Mol. Cell Biol.* **1999**, *19*(5), 3895-3903.
23. Johansson, L.; Bavner, A.; Thomsen, J. S.; Farnegardh, M.; Gustafsson, J. A.; Treuter, E. *Mol. Cell Biol.* **2000**, *20*(4), 1124-1133.
24. Marion, D.; Wuthrich, K. *Biochem. Biophys. Res. Commun.* **1983**, *113*(3), 967-974.
25. Rance, M.; Sorensen, O. W.; Bodenhausen, G.; Wagner, G.; Ernst, R. R.; Wuthrich, K. *Biochem. Biophys. Res. Commun.* **1983**, *117*(2), 479-485.
26. Piotto, M.; Saudek, V.; Sklenar, V. *J. Biomol. NMR* **1992**, *2*(6), 661-665.
27. Driscoll, P. C.; Gronenborn, A. M.; Beress, L.; Clore, G. M. *Biochemistry* **1989**, *28*(5), 2188-2198.
28. Wuthrich, K.; Billeter, M.; Braun, W. *J. Mol. Biol.* **1983**, *169*(4), 949-961.